

Dynamic Label Assignment for Object Detection by Combining Predicted and Anchor IoUs

Tianxiao Zhang[†], Ajay Sharda[‡], Bo Luo[†], Guanghui Wang^{*}

[†] Department of Electrical Engineering and Computer Science, University of Kansas, Lawrence KS, USA, 66045

[‡] Department of Biological and Agricultural Engineering, Kansas State University, Manhattan, Kansas, USA, 66506

^{*} Department of Computer Science, Ryerson University, Toronto ON, Canada, M5B 2K3

{tianxiao, bluoluo}@ku.edu, asharda@k-state.edu, wangcs@ryerson.ca

Abstract—Label assignment plays a significant role in modern object detection models. Detection models may yield totally different performances with different label assignment strategies. For anchor-based detection models, the IoU threshold between the anchors and their corresponding ground truth bounding boxes is the key element since the positive samples and negative samples are divided by the IoU threshold. Early object detectors simply utilize a fixed threshold for all training samples, while recent detection algorithms focus on adaptive thresholds based on the distribution of the IoUs to the ground truth boxes. In this paper, we introduce a simple and effective approach to perform label assignment dynamically based on the training status with predictions. By introducing the predictions in label assignment, more high-quality samples with higher IoUs to the ground truth objects are selected as the positive samples, which could reduce the discrepancy between the classification scores and the IoU scores, and generate more high-quality boundary boxes. Our approach shows improvements in the performance of the detection models with the adaptive label assignment algorithm and lower bounding box losses for those positive samples, indicating more samples with higher quality predicted boxes are selected as positives. The source code will be available at <https://github.com/ZTX-100/DLA-Combined-IoUs>.

I. INTRODUCTION

Object detection is a fundamental problem in computer vision that simultaneously classifies and localizes all objects in images or videos. With the fast development of deep learning, object detection has achieved great success and been applied to many real-world tasks such as object tracking [35][34], and image classification [3][24], segmentation [7][9], and medical image analysis [13].

Label assignment is to divide the samples into positives and negatives, which is essential to the success of object detection models. For anchor-based models, the core element for label assignment is the threshold for the division of positive samples and negative samples. After we calculate the intersection over union (IoU) between anchors and ground truth (GT) bounding boxes, the positive samples are those anchors whose IoUs are larger than the threshold, while others are negatives or ignored. The early detection models [28][20] utilize fixed threshold to divide the positives and negatives. However, the algorithms with a fixed threshold for dividing the positives and negatives ignore the differences between various ground truth bounding boxes for their shapes and sizes.

In recent years, several adaptive label assignment strategies have been proposed to adaptively calculate the threshold.

These algorithms adaptively select positive samples and negative samples based on the IoU distribution between anchors and ground truth bounding boxes so that the ground truth bounding boxes that have more high-quality anchors corresponding to them will have a higher IoU threshold and those which have the most low-quality anchors corresponding to them will have a low IoU threshold. Nevertheless, adaptive assignment methods do not assign positives and negatives based on the predictions which are more accurate to represent the training status. Due to the discrepancy between the classification and localization, classification scores cannot precisely correspond to the localization quality, while NMS (non-maximum suppression) supposes classification scores represent the localization quality and filters duplicates so that only the samples with high classification scores will be kept. However, if classification scores cannot accurately represent the localization quality, the high-quality bounding boxes might be eliminated and some low-quality bounding boxes might be kept. While fixed anchors cannot guarantee the quality of the predicted bounding boxes.

Therefore, introducing predictions to instruct label assignment is an effective approach to include the anchors which could generate high-quality predictions as the positives. There are uncertainties for predictions in the early training stage, so we cannot directly replace anchors with predicted bounding boxes. Adding distances to the ground truth centers as prior is proposed in some algorithm that utilizes predictions [39] to weight the positive samples. While the predictions (classification scores or IoU scores) and the distances are two different “domains” and they cannot be naturally combined. Autoassign [39] designed a center weighting module to solve this problem but the module might be sub-optimal due to the assumption that the samples closer to centers of GT would have more weights. “All-to-Top-1” [10] reduces the number of anchors in the bag based on iterations instead of predictions. Thus, the training might not be optimal since the number of anchors in the bag is not controlled by predictions and might not satisfy the training status.

We propose a simple and effective method that directly combines the predicted IoUs between the predicted bounding boxes and the ground truth bounding boxes, and the anchor IoUs between the anchors and the ground truth bounding boxes. According to the adaptive models, the adaptive thresh-

old is attained according to the statistical properties of the IoUs between the candidate anchors and the ground truth bounding boxes. While our method computes the distribution of the predicted IoUs and the anchor IoUs separately and then attains the combined parameters by simply adding them, respectively. Finally, the combined threshold is computed by the combined distribution parameters. Since the predictions in each iteration are involved in the label assignment, soft targets (predicted IoUs between the predicted bounding boxes and the ground truth boxes) are more appropriate than the hard target (label 1) for positives in classification loss. QFL [16] and VFL [32] are commonly utilized classification loss with soft target. Both of them could further boost the performance of our proposed method. In addition, we replace the Centerness branch with the IoU branch for better accuracy. The experiments on COCO dataset [19] illustrate the effectiveness of our method without extra cost.

II. RELATED WORKS

A. Object Detection

Object detection could be categorized as two-stage approaches and one-stage approaches [14][21][31]. Two-stage detection models [28][1][4][17] first employ region pyramid networks (RPN) [28] to select anchors with high possibility to have high IoUs with some ground truth objects and refine those candidate anchors. Then the refined anchors are fed into the second stage to be classified and further regressed. While one-stage detectors [20][25][26][27][18] directly classify and regress the anchors without selecting and refining some candidates. Two-stage detectors often yield higher accuracy but lower speed compared to one-stage counterparts. With the emergence of RetinaNet [18], the accuracy discrepancy between the one-stage and two-stage models has been reduced by introducing focal loss to suppress the loss of easy samples so that one-stage methods could achieve both high accuracy and low latency. Thus one-stage approaches are dominating current object detection models.

With the development of anchor-free models, the pre-defined anchors are no longer required for a well-performed detection model [12][5][38][40][29]. The anchor-free models either regress the bounding box from anchor points (feature points) [40][29] or predicts some special points of the ground truth object such as corners or extreme points of the boundary boxes of the objects [12][5][38] and finally constructs the predicted bounding boxes from those special points. Recently, some object detection models [2][37][41][22] are enhanced by attention modules with Transformers [30], which are originally invented for natural language processing. DETR [2] first introduces the Transformers to the head of detection models, which is also anchor free. Nonetheless, due to the global attentions utilized in Transformers and the large resolution of the images for object detection, DETR requires much longer epochs than its CNN counterparts to convergence. Thus recent algorithms [23][6] attempt to design fast training convergence DETR to speed up the training process.

B. Label Assignment

The label assignment is the core factor for the performance of the detection models and how to divide positive samples and negative samples would determine how the networks learn and converge. The early detection models such as Faster R-CNN [28], SSD [20] and RetinaNet [18] utilize traditional label assignment approaches with fixed thresholds for dividing positives and negatives. Even though those detection models with fixed thresholds are still effective for label assignment, they ignore the differences between various object samples for their shapes, sizes, and numbers of corresponding positive anchors. Recently, researchers focus on designing adaptive thresholds and gradually discard the fixed thresholds for label assignment. ATSS [33] computes the adaptive thresholds by calculating the mean and standard deviation according to the distribution of the IoUs between the candidate anchors and the ground truth objects. PAA [11] fits the candidate anchors into the Gaussian mixture model and separates them probabilistically.

Using predictions to guide the label assignment could be more accurate since the pre-defined anchors might not accurately reflect the actual training status. Nevertheless, predictions in the early training stage are inaccurate and unreasonable to instruct the label assignments. FreeAnchor [36] exploits maximum likelihood estimation (MLE) to model the training process so that each ground truth could have at least one corresponding anchor with both high classification score and localization score. MAL [10] employs predictions from classification and localization as the joint confidence for evaluation of the anchors. To alleviate the sub-optimal anchor-selection problem, MAL perturbs the features of selected anchors based on the joint confidence and proposes “All-to-Top-1” strategy for anchor selection. Autoassign [39] introduces center weighting as the prior to address the unreasonable predictions in the early training phase, which indicates that the samples closer to the centers of ground truth would have more weights.

III. PROPOSED APPROACH

A. Revisit Adaptive Label Assignment

The adaptive label assignment strategies frequently divide the positive and negative samples by calculating the statistical parameters (e.g. mean and standard deviation) based on the candidate anchors or anchor bags which are selected according to the Euclidean distances between the centers of the anchors to the centers of the ground truth bounding boxes. After the candidate anchors are selected based on their positions to the ground truth boxes, the adaptive thresholds are computed based on the distribution of their IoUs to the corresponding ground truth bounding boxes.

The adaptive algorithms for label assignment compute the thresholds adaptively according to the shapes and sizes of the GT bounding boxes. If the GT boxes are large or square-like, the threshold will be higher since there are more high-quality

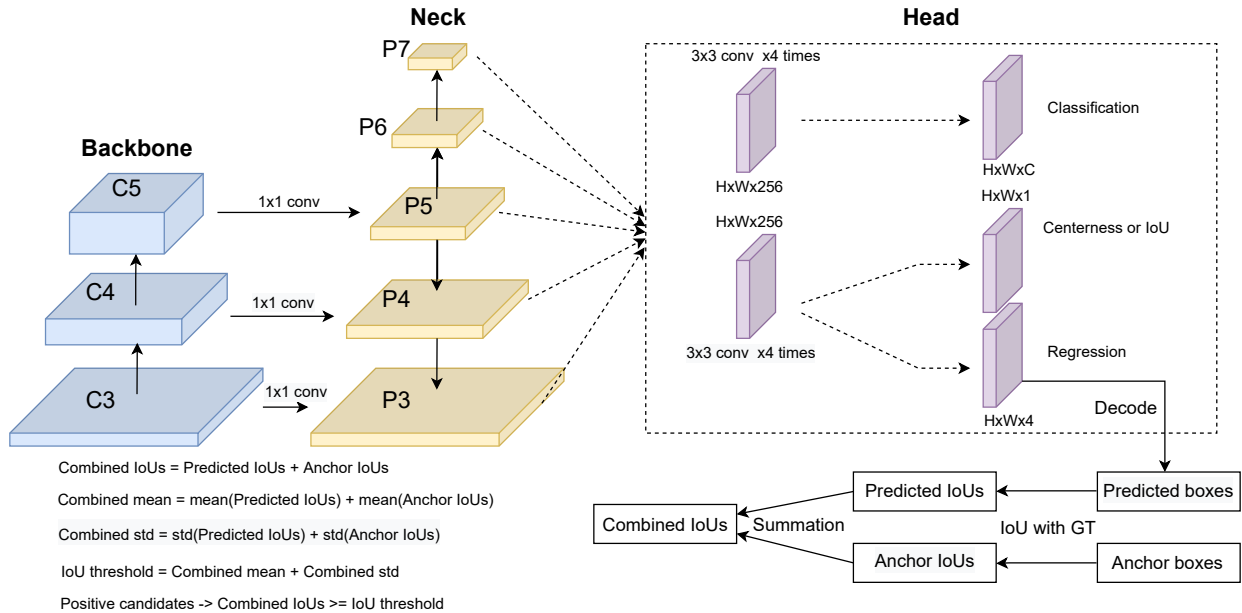


Fig. 1. The network structure of our model. The baseline structure of our model is the same as ATSS [33], which includes a CNN backbone [8], an FPN neck [17] and a head that has two branches for classification and regression, respectively. Our approach would employ the predicted boxes which are decoded from the regression branch and we select ATSS [33] as an adaptive example for label assignment. Then the predicted IoUs and the anchor IoUs are attained by calculating the IoUs between the predicted boxes and the GTs, and the IoUs between the anchor boxes and the GTs, respectively. Finally, the Combined IoUs (CIoUs) are computed by summing the predicted IoUs and the anchor IoUs. ATSS utilizes mean and standard deviation to compute the threshold, so the same calculation is implemented to attain the combined mean and combined std. The IoU threshold is computed by the summation of combined mean and combined std, and the positive candidates are defined as the samples whose Combined IoUs are larger than or equal to the IoU threshold. The positive candidates are restricted inside the ground truth bounding boxes as the final positive samples.

anchors corresponding to them. If the GT boxes are slender or small in shape, the threshold will be lower due to most low-quality anchors corresponding to them. Nevertheless, most adaptive methods only compute adaptive thresholds according to the relationship between anchors and the ground truth boxes. They merely rely on the pre-defined anchor boxes and ignore the predicted bounding boxes during the training process. In other words, the anchor with the highest IoU to the GT box cannot guarantee its predicted bounding box also have the highest IoU to the GT among all positive anchors. Thus some samples with high-quality predicted bounding boxes might be defined as negative samples whose classification target is 0. Thus the performance of high-quality bounding boxes is affected. Using predicted information may improve the accuracy for defining the positives and negatives since predictions can reflect the real training status of each sample. However, directly using the predictions may not be appropriate since the predictions in the early training stage are unreasonable to instruct the positive and negative definition. Thus, we propose a simple and effective approach to address this problem by combining the predicted IoUs to the ground truth and the pre-defined anchor IoUs to the ground truth for each training sample.

B. Dynamic Label Assignment

We propose a simple and effective dynamic label assignment strategy, which introduces the predictions to the anchor boxes

for label assignment. At the early training phase, the predictions are inaccurate due to the random initialization. Thus the anchors would act as prior to instruct the label definition. The predictions gradually dominate the combined IoUs and would lead the label assignment with the training proceeding and the predictions being improved. The network structure is illustrated in Figure 1. We use ATSS [33] as the base network, which has a CNN backbone [8], an FPN neck [17], and a shared head which has two branches for classification and regression, respectively. The proposed approach extracts the regression results and decodes the regression offsets to the coordinates of bounding boxes, and finally calculates the IoUs between the decoded bounding boxes and the GTs. The predicted IoUs will be combined with anchor IoUs for selecting the positive samples as demonstrated in Figure 1.

Why utilizing predictions is so important to guide the label assignment? The predictions are more accurate than the pre-defined anchors for defining the positives and negatives since we select the final results and implement the NMS algorithm based on the predicted results instead of the anchor boxes. We frequently design the detection models based on the assumption that the samples whose pre-defined boxes have high IoUs with the ground truth boxes are appropriate to be selected as positives or the samples whose centers are close to the centers of the ground truth objects are good candidates for positives. Once the positive samples are selected for each image, they would not be modified during the training process

since the pre-defined anchor boxes or anchor points are fixed and they would not be changed according to the training status. Nevertheless, the samples with high-quality predictions might not frequently be those samples with high-quality anchor boxes or anchor points, although they have higher probabilities to generate high-quality predictions.

If we force the samples with high-quality anchors boxes or anchor points to be the positives through the entire training process, the network would focus on learning those samples even though their predictions are not good enough and ignore the samples which could generate better predicted results but might be assigned as negatives due to the relatively low-quality anchor boxes or anchor points. While if the predictions are introduced in each iteration to assist the definition of positive samples and negative samples, we could select more samples with high-quality predictions as positives and further improve those samples. Adding predicted IoUs to anchor IoUs could yield better results and generate higher quality predictions. The anchor IoUs are also necessary for our approach due to the random initialization of the network and they can act as prior. In our method, the predictions and the prior are both IoUs to the ground truth bounding boxes, thus they can be naturally combined together by addition without any special design as shown in Figure 1.

C. Soft Targets for Classification Loss

With the emergence of focal loss [18], most modern object detection models exploit focal loss for learning the class labels. Focal loss addresses the extreme imbalance between the positive samples and negative samples during training and suppresses the majority of easy negative samples which could dominate the training loss due to the extremely large number of those easy negatives.

Due to the introduction of predictions for label assignment, using soft target (predicted IoUs to the ground truth boxes) is more appropriate to rank the high predicted IoUs on top of other low predicted IoUs, which is utilized in GFL [16] and VFNet [32]. GFL is comprised of QFL and DFL for classification and regression, respectively. We employ QFL for classification in our model. The cross-entropy loss of QFL is switched to the general form for positives since the soft targets are not equal to 1. In addition, the focal loss weights are also modified according to the soft targets.

Instead of down-weighting the losses when the classification predictions approach to the soft targets as used in QFL, VFNet [32] exploits VFL [32] that weights the positive losses with the soft targets to which those positives are assigned. By changing the weights to the IoU targets for positives, the losses of positive samples with higher IoU targets would also be higher so that the network could focus on learning those high-quality positives. In the experiments, we empirically illustrate that our proposed approach surpasses the same model using QFL or VFL in Table I. In addition, by combining our proposed method with QFL or VFL, the performance of the detection model could be further improved.

IV. EXPERIMENTS

Implementation Details: The experiments are conducted on COCO dataset [19], where *train2017* is employed for training and *val2017* is for validation and ablation study. The training strategy exploits scheduler 1x (90k iterations) for validation where the batch size is 16, and the initial learning rate is 0.01 and the learning rate is decreased by 0.1 at the 60k and 80k iterations. The images are resized so that the maximum length of the longer side is 1333 and the length of the shorter side is 800. ResNet-50 [8] is utilized for all ablation study.

A. Ablation Study

In the experiments, ATSS algorithm [33] is selected as an example to illustrate the effectiveness of our proposed approach. ATSS [33] employs the mean and standard deviation of the IoUs between the candidate anchors and the ground truth boxes to calculate the thresholds and select positive samples. We introduce the predicted IoUs to the ATSS algorithm (shown at the bottom of Figure 1) to demonstrate the effectiveness of our approach.

1) *The effectiveness of proposed method:* To prove the effectiveness of our proposed method, we conducted several experiments based on the ATSS structure. The experimental results are shown in Table I.

TABLE I
THE EFFECTIVENESS OF THE PROPOSED METHOD

| model | AP | AP50 | AP75 | APs | APm | APl |
|------------|--------------|-------|-------|-------|-------|-------|
| ATSS | 39.06 | 57.11 | 42.49 | 22.33 | 43.27 | 50.23 |
| ATSS+CIoUs | 39.75 | 57.43 | 43.08 | 23.03 | 43.83 | 52.27 |
| ATSS+QFL | 39.61 | 57.41 | 43.05 | 23.25 | 43.69 | 52.19 |
| ATSS+VFL | 39.65 | 57.38 | 43.39 | 23.45 | 43.53 | 52.19 |

From Table I, ATSS combined with our proposed CIoUs (Combined IoUs) surpasses the same model with soft targets (QFL and VFL) for classification loss. Our simple modification can boost the original ATSS algorithm by around 0.7 AP on the MS COCO *val2017* dataset, which demonstrates that using predictions could better guide the positive and negative definitions and the anchor boxes are also necessary for instructing the label assignment. By simply combining them together, the model could yield better accuracy improvement. We simply introduce CIoUs into ATSS here and the labeled target is still the hard target (1 for positives). In the following experiments, we will show that the performance could be further boosted with the soft target (QFL or VFL).

2) *The Contribution of Each Element:* In this section, we implement the experiments by removing some of the components. Through this ablation study, we can easily recognize the contribution of each element. The experimental results are demonstrated in Table II.

In Table II, AIoUs represent the IoUs between the pre-defined anchor boxes and the ground truth bounding boxes. If only AIoUs are selected, the original ATSS is implemented. PIoUs indicate the IoUs between the predicted bounding boxes

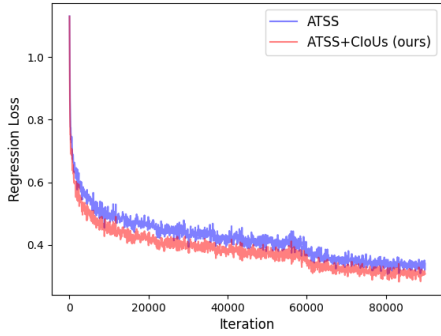


Fig. 2. The regression loss of ATSS and ATSS+CIoUs

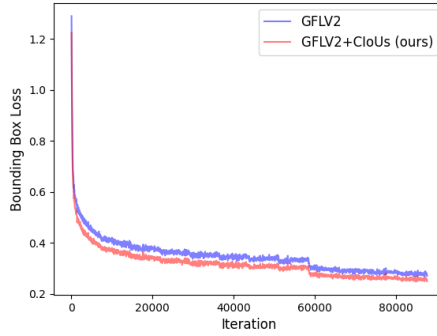


Fig. 3. The bounding box loss of GFLV2 and GFLV2+CIoUs

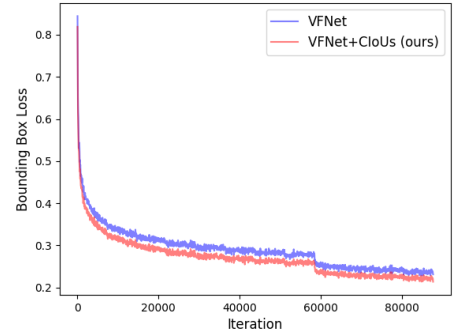


Fig. 4. The bounding box loss of VFNet and VFNet+CIoUs

TABLE II
THE ABLATION STUDY FOR EACH ELEMENT

| AIoUs | PIoUs | QFL | VFL | Centerness branch | IoU branch | AP | AP50 | AP75 | APs | APm | API |
|-------|-------|-----|-----|-------------------|------------|--------------|-------|-------|-------|-------|-------|
| ✓ | | | | ✓ | | 39.06 | 57.11 | 42.49 | 22.33 | 43.27 | 50.23 |
| | ✓ | | | ✓ | | 29.39 | 46.77 | 31.13 | 21.57 | 28.38 | 37.08 |
| ✓ | | | | ✓ | | 39.75 | 57.43 | 43.08 | 23.03 | 43.83 | 52.27 |
| ✓ | ✓ | ✓ | | ✓ | | 40.07 | 57.46 | 43.73 | 23.47 | 44.30 | 52.60 |
| ✓ | ✓ | | ✓ | ✓ | | 39.83 | 57.45 | 43.15 | 22.75 | 44.22 | 52.88 |
| ✓ | ✓ | ✓ | | | ✓ | 40.30 | 57.49 | 44.00 | 22.85 | 44.48 | 53.71 |
| ✓ | ✓ | | ✓ | | ✓ | 40.15 | 57.37 | 43.64 | 23.51 | 44.09 | 53.21 |

and the ground truth boxes. If both AIoUs and PIoUs are selected, our proposed Combined IoUs are implemented by summing the computed AIoUs and PIoUs. We can obviously notice that only employing PIoUs for label assignment significantly compromises the performance of the model from 39.06 AP to 29.39 AP, while simply adding the PIoUs to AIoUs for defining the positive samples and negative samples could yield around 0.7 AP improvement and the improvement happens in all metrics (AP, AP50, AP75, APs, APm, API).

Figure 2 illustrates the regression loss of the original ATSS and ATSS with our proposed combined IoUs. From Figure 2, the regression loss does not have too much difference at the early training phase for both models. While with the training process going on, our approach has lower regression loss than the original model, which indicates our model could select positive samples with higher quality bounding boxes since more accurate predicted bounding boxes would yield lower regression loss. Additionally, the average precision for large objects (API) is greatly improved the AP by about 2%.

From Table II, our proposed approach (AIoUs+PIoUs) could be further improved by soft targets (QFL or VFL). The original ATSS adopts centerness as the additional branch to weight the positive samples so that the samples closer to the centers of the GTs could have relatively higher weights than those far from the centers of the GTs. After switching the centerness to IoU (predicting IoU instead of centerness), the performance could be further boosted.

3) *Balancing Predicted IoUs and Anchor IoUs*: We also investigate how to balance the predicted IoUs and the anchor IoUs when calculating the dynamic thresholds. The experimental results are illustrated in Table III.

TABLE III
THE ABLATION STUDY ON THE WEIGHTS FOR COMBINATION

| PIoUs | AIoUs | AP | AP50 | AP75 | APs | APm | API |
|-----------------|-------------------|--------------|-------|-------|-------|-------|-------|
| 1 | 1 | 39.75 | 57.43 | 43.08 | 23.03 | 43.83 | 52.27 |
| 0.5 | 1 | 39.43 | 57.23 | 42.92 | 23.04 | 43.56 | 51.31 |
| 1.5 | 1 | 39.55 | 57.38 | 42.63 | 23.15 | 43.28 | 51.60 |
| 1 | 0.5 | 39.42 | 57.13 | 42.46 | 22.95 | 43.04 | 51.03 |
| 1 | 1.5 | 39.51 | 57.27 | 42.68 | 22.94 | 43.31 | 51.72 |
| D _{up} | 1 | 39.22 | 56.92 | 42.50 | 22.74 | 42.98 | 51.35 |
| 1 | D _{down} | 35.05 | 53.33 | 37.58 | 22.44 | 35.76 | 46.27 |
| D _{up} | D _{down} | 35.64 | 53.78 | 38.09 | 22.68 | 36.57 | 48.12 |

From Table III, we can see that the model with the ratio between PIoUs and AIoUs being 1:1 could yield the best accuracy. D_{up} indicates the dynamic weight which gradually increases the weight with the training proceeding. D_{down} represents the dynamic weight that gradually decreases the weight with the training proceeding. In the experiment, we utilize $iteration/max_iter$ as D_{up} and $(1 - iteration/max_iter)$ as D_{down}. In the representation, $iteration$ is the current iteration and max_iter represents the total iterations the training would implement.

In our experiments, we apply D_{up} to the predicted IoUs and D_{down} to the anchor IoUs so that the predicted IoUs would gradually take over the label assignment and the anchor IoUs would gradually fade out of the label assignment. Nonetheless, introducing the dynamic weights to PIoUs and AIoUs does not improve the performance and applying D_{down} to AIoUs greatly worsens the accuracy of the detection model, which verifies that anchors still play a significant role in our method. Since PIoUs would gradually increase with the training proceeding due to increasing localization

TABLE IV
EVALUATION RESULTS ON COCO TEST-DEV

| Method | Backbone | Scheduler | MStrain | AP | AP50 | AP75 | APs | APm | API |
|---------------------|----------------|-----------|---------|------|------|------|------|------|------|
| ATSS*[33] | ResNet-50 | 1x | | 39.2 | 57.5 | 42.6 | 22.3 | 41.9 | 49.0 |
| ATSS*[33] | ResNet-50-DCN | 1x | | 43.0 | 61.2 | 46.8 | 24.5 | 45.9 | 55.3 |
| ATSS[33] | ResNet-101 | 2x | ✓ | 43.6 | 62.1 | 47.4 | 26.1 | 47.0 | 53.6 |
| ATSS[33] | ResNet-101-DCN | 2x | ✓ | 46.3 | 64.7 | 50.4 | 27.7 | 49.8 | 58.4 |
| GFL[16] | ResNet-101 | 2x | ✓ | 45.0 | 63.7 | 48.9 | 27.2 | 48.8 | 54.5 |
| GFL[16] | ResNet-101-DCN | 2x | ✓ | 47.3 | 66.3 | 51.4 | 28.0 | 51.1 | 59.2 |
| Dynamic ATSS | ResNet-50 | 1x | | 40.3 | 57.9 | 44.1 | 22.5 | 43.6 | 51.2 |
| Dynamic ATSS | ResNet-50-DCN | 1x | | 44.4 | 61.9 | 48.6 | 25.1 | 47.8 | 58.1 |
| Dynamic ATSS | ResNet-101 | 2x | ✓ | 44.7 | 62.5 | 48.9 | 26.7 | 48.3 | 55.7 |
| Dynamic ATSS | ResNet-101-DCN | 2x | ✓ | 47.3 | 65.0 | 51.7 | 28.3 | 50.8 | 60.4 |

TABLE V
APPLICATION OF PROPOSED APPROACH TO STATE-OF-THE-ART MODELS

| model | AP | AP50 | AP75 | APs | APm | API |
|-------------|-------------|------|------|------|------|------|
| GFLV2 | 40.6 | 58.1 | 44.4 | 22.9 | 44.2 | 52.6 |
| GFLV2+CIoUs | 41.1 | 58.6 | 44.8 | 23.7 | 44.3 | 53.9 |
| VFL | 41.3 | 59.2 | 44.8 | 24.5 | 44.9 | 54.2 |
| VFL+CIoUs | 41.6 | 59.5 | 44.9 | 24.3 | 45.1 | 54.6 |

accuracy of predicted boxes, dynamic weight has no positive effect on PIoUs. In our experiments, a simple summation of PIoUs and AIoUs is applied and no weights are utilized for combining them. This ablation study also demonstrates that anchor IoUs and predicted IoUs could be naturally combined together without any sophisticated formula or weights, which is simpler than using a complicated formula to combine the distances to GT centers and the predictions [39] or “All-to-Top-1” [10] that gradually decreases the number of the anchors in the bag.

B. Application to the State-of-the-Art

The proposed approach could be applied to other state-of-the-art models that employ the ATSS algorithm for label assignment by combining the predicted IoUs with the anchor IoUs. We have also applied our strategy to the most recent GFLV2 [15] and VFNet [32] detection models. Instead of directly predicting the offsets of the bounding boxes, GFLV2 [15] designs a distribution-guided quality predictor to estimate the localization quality via the bounding box distributions, and VFNet [32] further implements bounding box refinement by proposing a star-shaped box feature representation. The performance of our approach on GFLV2 [15] and VFNet [32] are shown in Table V.

From Table V we can see that, after applying our proposed method to the GFLV2 and VFNet, the two state-of-the-art models are further improved on COCO *val2017*. Figure 3 and Figure 4 illustrate and compare the bounding box losses of GFLV2 to GFLV2+CIoUs, and VFNet to VFNet+CIoUs, respectively. Similar to the experiments on ATSS, the models with our approach yield lower bounding box losses with the training proceeding, which demonstrates our proposed

method could help the detection models to select higher quality predicted bounding boxes that have lower bounding box losses.

C. Evaluation on COCO test-dev

We apply our dynamic label assignment strategy (CIoUs+QFL+IOU branch) to the COCO *test-dev* [19] and compare them with the original ATSS. Table IV illustrates the experimental results of the state-of-the-art models and our methods, where “MStrain” indicates multi-scale training strategy and “*” denotes our re-implementation.

The experiments demonstrate that our strategy could boost the original ATSS by more than 1 mAP and 2 AP for large objects with various backbones and training strategies. We also notice that our results are competitive to the state-of-the-art GFL [16], which is also based on ATSS. While due to the introduction of the distribution focal loss (DFL), GFL [16] predicts the bounding boxes multiple times for each sample to estimate the localization quality, which would increase the number of parameters. While our model is more efficient without introducing extra parameters and computational costs. It directly predicts the 4 offsets of the bounding boxes as the original ATSS model.

V. CONCLUSION

In this paper, we have illustrated the advantages of using predictions for defining positive samples and negative samples for object detection models, and proposed a simple and effective strategy to improve the performance of the adaptive algorithm for label assignment by combining the predicted IoUs and anchor IoUs so that the adaptive algorithm could divide the positive and negative samples dynamically according to the predictions. By introducing the predicted IoUs that could be combined with the anchor IoUs by summation, the dynamic algorithm for label assignment could implement label assignment based on the training status and select the samples with higher quality predicted bounding boxes as the positives. When our method is applied to state-of-the-art detection models, the performance of the models could be further improved. The simple and effective approach could inspire more work on designing dynamic object detectors based on the training status.

REFERENCES

- [1] Z. Cai, Q. Fan, R. S. Feris, and N. Vasconcelos, "A unified multi-scale deep convolutional neural network for fast object detection," in *European conference on computer vision*. Springer, 2016, pp. 354–370.
- [2] N. Carion, F. Massa, G. Synnaeve, N. Usunier, A. Kirillov, and S. Zagoruyko, "End-to-end object detection with transformers," in *European Conference on Computer Vision*. Springer, 2020, pp. 213–229.
- [3] F. Cen, X. Zhao, W. Li, and G. Wang, "Deep feature augmentation for occluded image classification," *Pattern Recognition*, vol. 111, p. 107737, 2021.
- [4] J. Dai, Y. Li, K. He, and J. Sun, "R-fcn: Object detection via region-based fully convolutional networks," in *Advances in neural information processing systems*, 2016, pp. 379–387.
- [5] K. Duan, S. Bai, L. Xie, H. Qi, Q. Huang, and Q. Tian, "Centernet: Keypoint triplets for object detection," in *Proceedings of the IEEE/CVF International Conference on Computer Vision*, 2019, pp. 6569–6578.
- [6] P. Gao, M. Zheng, X. Wang, J. Dai, and H. Li, "Fast convergence of detr with spatially modulated co-attention," *arXiv preprint arXiv:2101.07448*, 2021.
- [7] K. He, G. Gkioxari, P. Dollár, and R. Girshick, "Mask r-cnn," in *Proceedings of the IEEE international conference on computer vision*, 2017, pp. 2961–2969.
- [8] K. He, X. Zhang, S. Ren, and J. Sun, "Deep residual learning for image recognition," in *Proceedings of the IEEE conference on computer vision and pattern recognition*, 2016, pp. 770–778.
- [9] L. He, J. Lu, G. Wang, S. Song, and J. Zhou, "Sosd-net: Joint semantic object segmentation and depth estimation from monocular images," *Neurocomputing*, vol. 440, pp. 251–263, 2021.
- [10] W. Ke, T. Zhang, Z. Huang, Q. Ye, J. Liu, and D. Huang, "Multiple anchor learning for visual object detection," in *Proceedings of the IEEE/CVF Conference on Computer Vision and Pattern Recognition*, 2020, pp. 10 206–10 215.
- [11] K. Kim and H. S. Lee, "Probabilistic anchor assignment with iou prediction for object detection," in *Computer Vision—ECCV 2020: 16th European Conference, Glasgow, UK, August 23–28, 2020, Proceedings, Part XXV 16*. Springer, 2020, pp. 355–371.
- [12] H. Law and J. Deng, "Cornernet: Detecting objects as paired keypoints," in *Proceedings of the European conference on computer vision (ECCV)*, 2018, pp. 734–750.
- [13] K. Li, M. I. Fathan, K. Patel, T. Zhang, C. Zhong, A. Bansal, A. Rastogi, J. S. Wang, and G. Wang, "Colonoscopy polyp detection and classification: Dataset creation and comparative evaluations," *arXiv preprint arXiv:2104.10824*, 2021.
- [14] K. Li, W. Ma, U. Sajid, Y. Wu, and G. Wang, "Object detection with convolutional neural networks," in *Deep Learning in Computer Vision*. CRC Press, 2020, pp. 41–62.
- [15] X. Li, W. Wang, X. Hu, J. Li, J. Tang, and J. Yang, "Generalized focal loss v2: Learning reliable localization quality estimation for dense object detection," in *Proceedings of the IEEE/CVF Conference on Computer Vision and Pattern Recognition*, 2021, pp. 11 632–11 641.
- [16] X. Li, W. Wang, L. Wu, S. Chen, X. Hu, J. Li, J. Tang, and J. Yang, "Generalized focal loss: Learning qualified and distributed bounding boxes for dense object detection," *arXiv preprint arXiv:2006.04388*, 2020.
- [17] T.-Y. Lin, P. Dollár, R. Girshick, K. He, B. Hariharan, and S. Belongie, "Feature pyramid networks for object detection," in *Proceedings of the IEEE conference on computer vision and pattern recognition*, 2017, pp. 2117–2125.
- [18] T.-Y. Lin, P. Goyal, R. Girshick, K. He, and P. Dollár, "Focal loss for dense object detection," in *Proceedings of the IEEE international conference on computer vision*, 2017, pp. 2980–2988.
- [19] T.-Y. Lin, M. Maire, S. Belongie, J. Hays, P. Perona, D. Ramanan, P. Dollár, and C. L. Zitnick, "Microsoft coco: Common objects in context," in *European conference on computer vision*. Springer, 2014, pp. 740–755.
- [20] W. Liu, D. Anguelov, D. Erhan, C. Szegedy, S. Reed, C.-Y. Fu, and A. C. Berg, "Ssd: Single shot multibox detector," in *European conference on computer vision*. Springer, 2016, pp. 21–37.
- [21] W. Ma, Y. Wu, F. Cen, and G. Wang, "Mdfn: Multi-scale deep feature learning network for object detection," *Pattern Recognition*, vol. 100, p. 107149, 2020.
- [22] W. Ma, T. Zhang, and G. Wang, "Miti-detr: Object detection based on transformers with mitigatory self-attention convergence," *arXiv preprint arXiv:2112.13310*, 2021.
- [23] D. Meng, X. Chen, Z. Fan, G. Zeng, H. Li, Y. Yuan, L. Sun, and J. Wang, "Conditional detr for fast training convergence," in *Proceedings of the IEEE/CVF International Conference on Computer Vision*, 2021, pp. 3651–3660.
- [24] K. Patel and G. Wang, "A discriminative channel diversification network for image classification," *Pattern Recognition Letters*, vol. 153, pp. 176–182, 2022.
- [25] J. Redmon, S. Divvala, R. Girshick, and A. Farhadi, "You only look once: Unified, real-time object detection," in *Proceedings of the IEEE conference on computer vision and pattern recognition*, 2016, pp. 779–788.
- [26] J. Redmon and A. Farhadi, "Yolo9000: better, faster, stronger," in *Proceedings of the IEEE conference on computer vision and pattern recognition*, 2017, pp. 7263–7271.
- [27] —, "Yolov3: An incremental improvement," *arXiv preprint arXiv:1804.02767*, 2018.
- [28] S. Ren, K. He, R. Girshick, and J. Sun, "Faster r-cnn: Towards real-time object detection with region proposal networks," *Advances in neural information processing systems*, vol. 28, pp. 91–99, 2015.
- [29] Z. Tian, C. Shen, H. Chen, and T. He, "Fcos: Fully convolutional one-stage object detection," in *Proceedings of the IEEE/CVF international conference on computer vision*, 2019, pp. 9627–9636.
- [30] A. Vaswani, N. Shazeer, N. Parmar, J. Uszkoreit, L. Jones, A. N. Gomez, L. Kaiser, and I. Polosukhin, "Attention is all you need," in *Advances in neural information processing systems*, 2017, pp. 5998–6008.
- [31] W. Xu, Y. Wu, W. Ma, and G. Wang, "Adaptively denoising proposal collection for weakly supervised object localization," *Neural Processing Letters*, vol. 51, no. 1, pp. 993–1006, 2020.
- [32] H. Zhang, Y. Wang, F. Dayoub, and N. Sunderhauf, "Varifocalnet: An iou-aware dense object detector," in *Proceedings of the IEEE/CVF Conference on Computer Vision and Pattern Recognition*, 2021, pp. 8514–8523.
- [33] S. Zhang, C. Chi, Y. Yao, Z. Lei, and S. Z. Li, "Bridging the gap between anchor-based and anchor-free detection via adaptive training sample selection," in *Proceedings of the IEEE/CVF conference on computer vision and pattern recognition*, 2020, pp. 9759–9768.
- [34] T. Zhang, X. Zhang, Y. Yang, Z. Wang, and G. Wang, "Efficient golf ball detection and tracking based on convolutional neural networks and kalman filter," *arXiv preprint arXiv:2012.09393*, 2020.
- [35] X. Zhang, T. Zhang, Y. Yang, Z. Wang, and G. Wang, "Real-time golf ball detection and tracking based on convolutional neural networks," in *2020 IEEE International Conference on Systems, Man, and Cybernetics (SMC)*. IEEE, 2020, pp. 2808–2813.
- [36] X. Zhang, F. Wan, C. Liu, R. Ji, and Q. Ye, "Freeanchor: Learning to match anchors for visual object detection," *arXiv preprint arXiv:1909.02466*, 2019.
- [37] M. Zheng, P. Gao, R. Zhang, K. Li, X. Wang, H. Li, and H. Dong, "End-to-end object detection with adaptive clustering transformer," *arXiv preprint arXiv:2011.09315*, 2020.
- [38] X. Zhou, J. Zhuo, and P. Krahenbuhl, "Bottom-up object detection by grouping extreme and center points," in *Proceedings of the IEEE/CVF Conference on Computer Vision and Pattern Recognition*, 2019, pp. 850–859.
- [39] B. Zhu, J. Wang, Z. Jiang, F. Zong, S. Liu, Z. Li, and J. Sun, "Autoassign: Differentiable label assignment for dense object detection," *arXiv preprint arXiv:2007.03496*, 2020.
- [40] C. Zhu, Y. He, and M. Savvides, "Feature selective anchor-free module for single-shot object detection," in *Proceedings of the IEEE/CVF Conference on Computer Vision and Pattern Recognition*, 2019, pp. 840–849.
- [41] X. Zhu, W. Su, L. Lu, B. Li, X. Wang, and J. Dai, "Deformable detr: Deformable transformers for end-to-end object detection," *arXiv preprint arXiv:2010.04159*, 2020.